Hindawi
Journal of Nanomaterials
Volume 2022, Article ID 2842861, 9 pages
https://doi.org/10.1155/2022/2842861

Research Article

Silicon Wearable Body Area Antenna for Speech-Enhanced IoT and Nanomedical Applications

N. Arun Vignesh,[1] Ravi Kumar,[2] R. Rajarajan,[3] S. Kanithan,[4] E. Sathish Kumar,[5] Asisa Kumar Panigrahy,[1] and Selvakumar Periyasamy[6]

[1]*Department of Electronics and Communication Engineering, Gokaraju Rangaraju Institute of Engineering and Technology, Hyderabad 500090, India*
[2]*Department of Electronics and Communication Engineering, Jaypee University of Engineering and Technology, Guna 473226, India*
[3]*Department of Electrical and Electronics Engineering, MVJ College of Engineering, Bangalore 560067, India*
[4]*Department of Electronics and Communication Engineering, MVJ College of Engineering, Bangalore 560067, India*
[5]*Department of Electronics and Communication Engineering, Gnanamani College of Technology, Namakkal, India*
[6]*Department of Chemical Engineering, School of Mechanical, Chemical and Materials Engineering, Adama Science and Technology University, Adama 1888, Ethiopia*

Correspondence should be addressed to Selvakumar Periyasamy; selvakumar.periyasamy@astu.edu.et

Received 31 March 2022; Revised 20 April 2022; Accepted 7 May 2022; Published 23 May 2022

Academic Editor: Samson Jerold Samuel Chelladurai

Copyright © 2022 N. Arun Vignesh et al. This is an open access article distributed under the Creative Commons Attribution License, which permits unrestricted use, distribution, and reproduction in any medium, provided the original work is properly cited.

We propose in this paper a reduction in the size of wearable antennas on silicon (Si) for medicinal frameworks and Internet of things (IoT) in various nanoapplications. This research also introduces one more type of dynamic patch antenna designed in favor of speech-enhanced healthcare applications. The most significant impediment to the adoption of smart correspondence and medical services frameworks is voice-enabled IoT. The primary objective of a body area network (BAN) is to give ceaselessly clinical information to the doctors. Actually, wireless body area network is flexible, dense, trivial, and less expensive. On the other hand, the main disadvantage is low efficiency for small printed antenna. Microstrip silicon antenna recurrence is changed because of ecological conditions, distinctive reception apparatus areas, and diverse framework activity modes. By using tunable antenna, the efficiency of bandwidth usage can be increased. Amplifiers are associated with the feed line of antenna in order to build its dynamic range. In this study, a dynamic polarized antenna is constructed, analysed, and attempted for fabrication. The gain of the antenna is 13 ± 2 dB for the frequency range of 390 to 610 MHz. The output of the polarized antenna is roughly 19 dBm. At different environmental conditions, the performance and ability to control the antenna could vary. To achieve stable performance, we have used varactor diode and voltage-controlled diode. This silicon wearable antenna can be fabricated and tested for many medical applications like health monitoring system and pacemakers. Furthermore, micromachining techniques can be used to lower the practical dielectric constant of silicon and hence improve radiation efficiency.

1. Introduction

Wearable frameworks have a few applications in close to home specialized device and clinical device as introduced in [1–6]. A preprint has previously been published [7]. WBAN and healthcare systems frequently use printed antennas in wearable applications [8, 9]. Printed antennas are also cost-effective, flexible, and can be utilized in many medical and IoT applications. These antennas are analysed and studied in [10–14]. Examination of radio transmission that occurs when a wearable antenna is working near a human system has been analysed in [15–20]. Notwithstanding, little printed antennas experience the ill effects of low productivity [21–24]. Dynamic reception apparatuses for correspondence frameworks are introduced in [25–31]. This research introduces a unique dynamic and tunable wireless antenna for WBAN applications. Acquiring and

transmitting information, as well as healthcare setups, could benefit from dynamic patch silicon antennas. Accepting antenna is related with a low noise intensifier in destination channels. The application and uses of silicon to fabricate a patch has also been analysed [32]. The increase in the dynamic circle radio wire is 26 ± 2.6 dB at frequency ranges from 360 to 590 MHz. The dynamic circle receiving wire commotion recurrence goes from 410 to 910 MHz and is 0.75 ± 0.25 dB. In different locations, the electric parameter should be monitored by varactor diode [31]. All of the dynamic antenna and devices discussed in this study are based on an acceptable interpretation of the recorded and estimated values.

2. Wearable Technology

The physiological boundaries of a patient are ceaselessly checked by a far-off observing station with the assistance of wearable receiving antenna. This observing framework implants a variety of sensors in the body. The sensors are put in a specific location and linked to the information-gathering architecture in standard wearable properties. In any event, the texturing links pick up commotion from power line obstacles, signals from adjacent transmitting sources, and the biological parameters are harmed as a result. When the texture is incorporated, repositioning is exceptionally troublesome. Progressively, number of sensors is coordinated into the texture to frame a system (Personal Area Network) and associates with the human framework to procure and send the physiological information to a wearable information obtaining framework. Wearable antennas can be made from microstrip antennas. In the last 20 years, patch antennas are being discussed widely in various articles. Users of mobile devices, Internet of Things, vehicles, and diagnostic implants could all benefit from printed antennas. This can be an excellent alternative for some of the nonwearable high radiating sensitive antennas. For VSWR greater than 2 : 1, few of the printed dipole antennas have very narrow bandwidth of around one percent. The dipole can be anything from a quarter to a half wavelength in length. Wearable innovation can be predicted in the next few years, as there are more studies being conducted in the subject due to strong demand.

3. Signatures of Body Area Network

3.1. Wearable Body Area Network (BAN) and Antenna. The dynamic antenna is a device that consolidates antennas with dynamic segments, as shown in this study. The emanating component is intended to give the ideal burden to the active components. The antenna and dynamic segments were reconciled, which drastically reduced the coordinating system's volume, complexity, and weight. The dynamic antenna has been used in wireless and clinical correspondence systems in the last few years [25–31]. The significant utilization of dynamic antenna is electronically filtering clusters and staged exhibits. At times, half and half electromechanical exhibits, consolidating mechanical controlling with electrical directing forming, are utilized.

By limiting electrical inspection to only single plane, this method is widely utilized to reduce the number of dynamic parts. It is particularly common for compact interfaces, where azimuth filtering is accomplished through pneumatic disturbance as well as rising capability is determined via a direct ordered display. Staged clusters are a lot quicker for bar exchanging than precisely checked antenna. Early staged cluster antenna was latent reception apparatuses. The front finish of the antenna was made out of cluster components with stage shifters. Strong enhancers with close to zero amplifiers can be attached to each radiating section and placed close towards the front end. The staged cluster engineering permits noteworthy force improvement and better productivity. Power dividers, phase changers, and oscillators may be included in the enhancer modules. Compact spectrum dynamic reception apparatuses could benefit the overall presentation of smart setups. In this work, the radiation pattern, bandwidth, and frequency response of the dual-polarized antenna and printed silicon wearable patch antenna are analysed.

4. WBAN with Loop Antenna

In Figure 1, the block diagram of the receiving antenna section of speech-enhanced IoT is shown which is the fundamental piece of the reception apparatus. A business E PHEMT LNA, a low commotion intensifier, is associated with the printed circle antenna. On a silicon wafer with a layer of .005 mm, the circle gathering contraption is etched with antenna breadth of 50 mm.

Through an information coordinating system, the emitting component is linked to the LNA. A yield coordinating system interfaces the speaker yield port to the recipient. Low noise amplifier frequency range is 0.45 to 3.5 GHz and gain is 25 dB to 0.3 GHz; maximum input power is 18 dBm at the time of operating temperature is -40°C to -80°C; storage temperature is -45°C to -90°C.

4.1. Active WBAN with Dual-Polarized Antenna. Figure 2 shows an active wearable body area network with double polar transmitter, which has since been introduced on [1]. On a 0.3 mm wide silicon dielectric substrate, the antenna feed arrangement is imprinted. Followed by the substrate, an emanating component of 0.3 mm thickness is imprinted. Finally, the thickness of the antenna is 0.006 mm and its size is 50 × 50 mm.

4.2. Active Transmitting WBAN with Dual-Polarized Antenna. The ports and S_{ij} parameters of dual-polarized antenna are shown Figure 3. The antenna level of length, breadth, and thickness, respectively, is 50 mm × 50 mm × 0.005 mm. The transmitting component is associated with the HPA by means of a yield HPA coordinating system. The HPA input coordinating system associates the enhancer port to the transmitter. At 410 to 450 MHz, the flexible communicative dual dipole antenna's S_{11} boundaries have been evaluated and estimated to be 3 : 1. In Figure 4(a), the WBAN block diagram of sending antenna with level oscillator, control and dynamic control unit is shown. The dual-polarized antenna has a gain of roughly 17 dBm. In Figure 4(b), the WBAN with active transmitting antenna is shown.

High-power amplifier frequency range is 0.5 to 3.5 GHz and gain is 16 dB to 0.5 GHz; maximum input power is

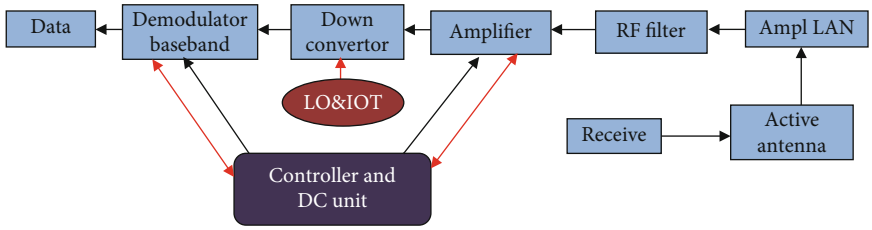

Figure 1: Receiving antenna with IoT.

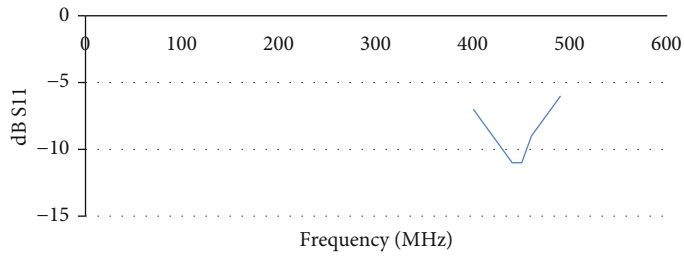

Figure 2: Frequency vs. dB S11 human body 25 dB to 90 MHz.

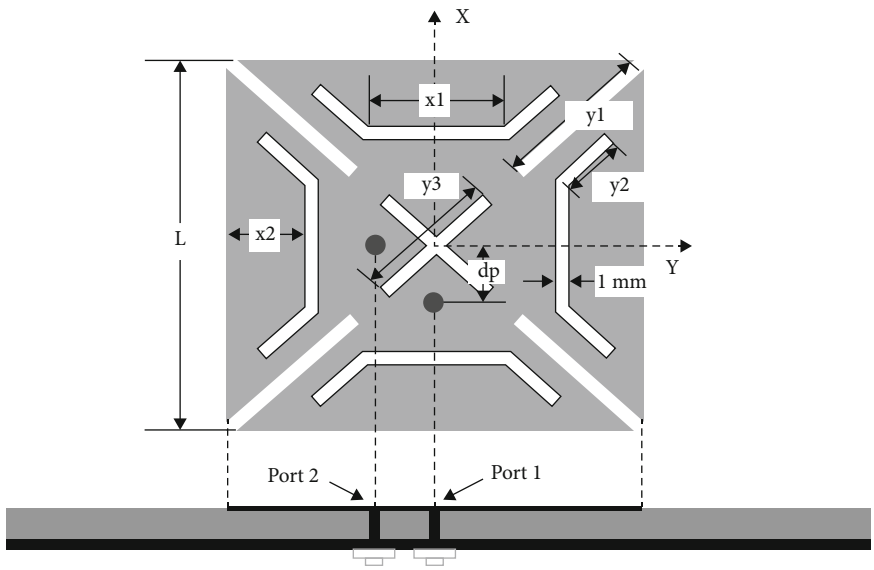

Figure 3: Two ports of the polarized antenna.

12 dBm at the time of operating temperature is -40°C to -80°C; storage temperature is -60°C to -100°C.The output of the dual-polarized transmitting antenna around 12 dBm is shown in Figure 4(c) and the resonant frequency curve versus capacitance is shown in Figure 4(d).

4.3. Wearable Body Area Network for Medical Application. A wearable material CPW antenna is accommodated Medical Body Area Network (MBAN) programs at 2 GHz, in light of on an electromagnetic band-hole structure and recurrence-specific surface. Without EBG-FSS, the essential reception apparatus has unidirectional radiation design, and keeping in mind that worked near human tissue, the general execution and productivity corrupt, and there is an unnecessary Specific Absorption Rate. To overcome this problem, the antenna contains EBG-FSS which lessens the retrogressive radiation, with SAR diminished by method of 95.5%. The preferred position is improved to 6.6 dBi and the front to returned proportion is improved with the guide of thirteen dB when contrasted with the essential receiving antenna. The overall components of the included structure are $50 \times 50 \times 2.4\,\text{mm}^3$. Recreation and test considerations show that the receiving wire coordinated with EBG-FSS can endure stacking by method of human tissue not withstanding twisting. Consequently, the structure is a decent possibility for MBAN programs.

A conservative conformal wearable CPW reception apparatus utilizing EBG-FSS for Medical Body Area Network bundles at 2.4 GHz is provided. The radio wire and EBG-FSS are

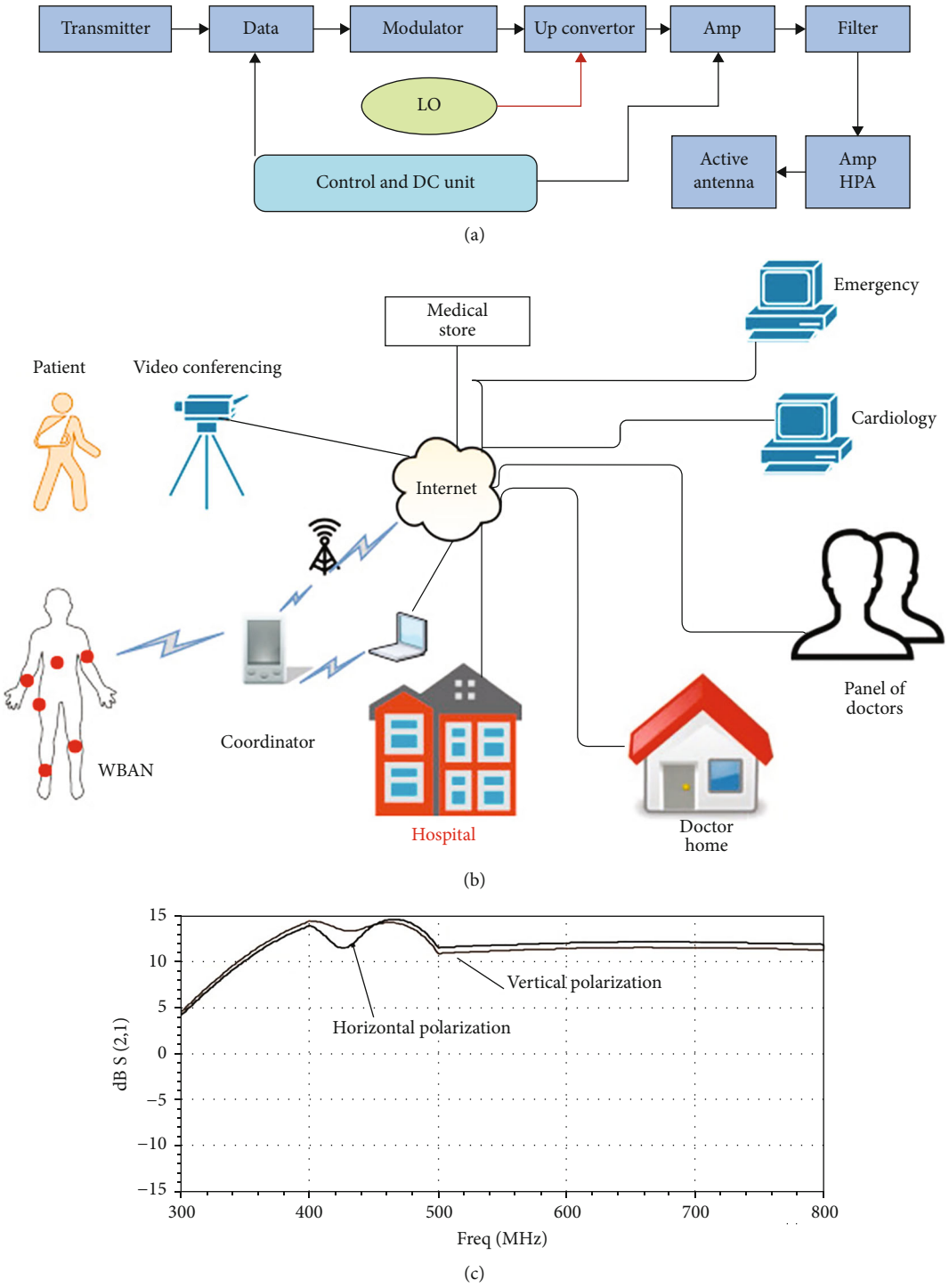

Figure 4: Continued.

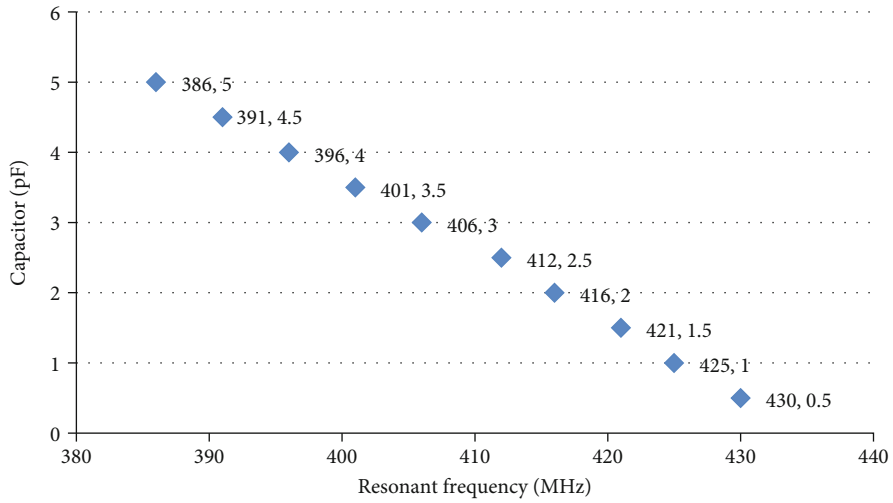

(d)

Figure 4: (a) WBAN block diagram of transmitting antenna. (b) Wireless body area network with active transmitting antenna. (c) Frequency vs. dB curve of active dual-polarized antenna. (d) CPW resonance frequency vs. capacitor.

planned dependent on texture substances that can be incorporated with our step-by-step garments. The antenna becomes concentrated in free territory, on multilayer model tissues and on a genuine body. The results show that when a receiving wire all alone, without EBG-FSS, is stacked with the guide of human tissue, the recurrence detunes: the reception apparatus plays inadequately because of the lossy human tissues. Besides, the reception apparatus creates a high charge of SAR that surpasses as far as possible, because of its unidirectional radiation test resulting in huge in reverse radiation. For the mentioned frequency, the specific absorption rate received is far below the recommended range as the body area is integrating the CPW radio wire with an EBG-FSS structure which presents disengagement among the body and the receiving wire. Along these lines, the detuning because of human edge stacking and furthermore the results of twisting are definitely diminished. Besides, the impacts show that the FBR is ventured forward with the guide of thirteen dB, the bit of leeway by methods for 6.55 dBi and the SAR diminished with the guide of extra than 95.5% when contrasted with the reception apparatus alone. Thusly, the offered CPW antenna is good for medical body area network.

4.4. Design and Antenna Performance. So as to think about the variety in designing antenna with desirable impedance matching, a design that imitates a helix structure is chosen at receiving side. The radiation effect over the human body had to be kept in consideration rather than the structure. A compact structure with 9 turns is shown in Figure 5. The microstrip is insulated with copper and it resembles the helix structure, and hence, it could receive the signals from the system that has been fixed over the human body. It has reduced interference and adjustable radiation with power. The received signals are to be processed as shown in the receiving antenna block diagram of Figure 1. The system can then be linked to IoT and medical systems where again the signals can be studied and proper treatment can

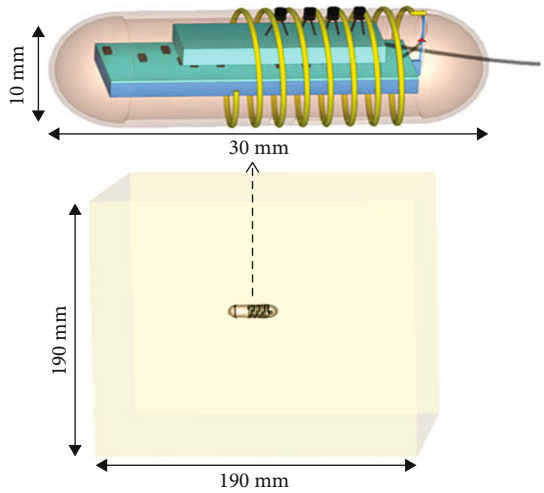

Figure 5: Antenna setup.

be given. With respect to design, a strip line has been planted on RO4003 with thickness ranging from 10 to 30 mm.

At the frequency range of 450 MHz to 460 MHz, the antenna has a VSWR over 3 : 1 and with antenna measurement of $40 \times 40 \times 6$mm. Figure 6 represents S_{11} boundaries over the human skin. If there is wind intrusion between the antenna and body, there could be an approximate expansion in the size from 0 mm to 1 mm. In this way, the dislocation of the reception apparatus could be anywhere between 0 and 3 percent. Though this will not affect the performance, it should be considered as it can lead to undesirable signal interventions which could anyway be removed with necessary filters. The design and performance analysis is carried out with the help of computer simulation technology software. As we analyse the dB with frequency, it has been found that with increase in the frequency the S_{11} decreases. As the desirable reflection coefficient represented as S_{11} parameter

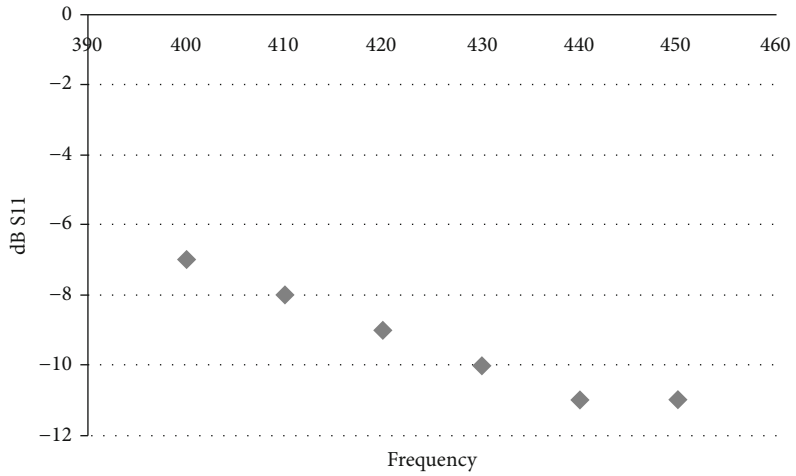

Figure 6: Measured S11 human body.

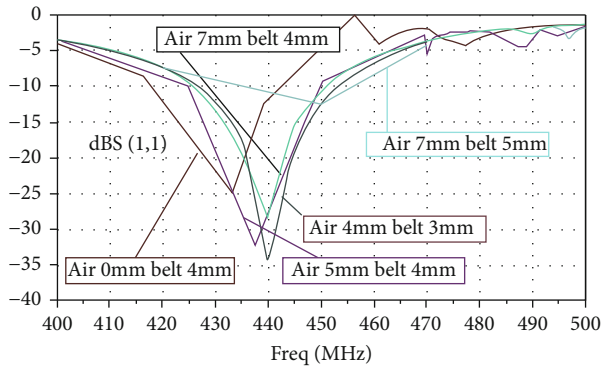

Figure 7: WBAN framework in air medium.

is around -11 to -13 dB, the values obtained at 420-450 MHz are promising with the values of -10 dB to -12 dB. This study shows that over human body, the antenna will be able to transmit with reflection coefficient of -11 dB.

4.5. Change of S_{11} Parameter from the Human Body. Advanced design system coding was used to analyse the antenna's insertion loss, which acts on the body with minimal distance from the surface. Figure 7 represents the S_{11} analysis of the distinctive strap and chemise depth, in addition to space separation amid radio wires with the person. The *s*-parameters represent the impedance match and mismatch. Here, we have obtained *s*-parameters with the help of a computer simulation technology tool. On the off chance, space separation was found to be expanded around 4 mm. There is acceptable understanding among estimated and determined outcomes. The volt control varactor might be utilized for tuning receiving wire resounding recurrence because of various radio wire areas put over the person.

4.6. Far-Field Analysis. The force flexibility for these segments should be kept to a minimum, and they should be light and robust. Distributed computing administrations are used to evaluate and validate information gathered from the far field. Also, speech-enhanced silicon patch can communicate data with clinical center, as well as back it to consumers. Clinical centers, patients, doctors, and sports centers all benefit from remote correspondence systems because they allow continuous estimating and observation of clinical data. The far-field analysis shows that the wearable wellbeing checking frameworks, as appeared in Figure 8, permit the radiation to intently follow changes in significant wellbeing boundaries and give criticism to keeping up ideal wellbeing status at each area of the body. The principle objective of WBANs is to persistently give biofeedback information. WBANs with such radiation pattern can pass information and can record electrocardiograms and measure internal heat level, circulatory strain, vessel pulse, and some social boundaries effectively. Body Area Network (BANs) incorporates various advantages with specialized gadgets utilizing the remote systems. The remote body zone system is a specific purpose remote sensor system that integrates multiple systems and remote gadgets to enable remote checking under diverse settings. In clinical focuses, such systems can be used with silicon-fabricated body antenna where states of an enormous number of patients can be continually observed.

Human wellbeing monitoring is becoming an increasingly important use of implanted sensor systems. A WBAN can monitor basic indicators, providing constant input for a variety of patient diagnostics procedures that rely on constant observation in changing situation and help in the process of patient's recovery.

4.7. Fabrication Flow of Silicon Wearable Body Area Antenna. The silicon wearable body area antenna can be fabricated using inkjet printing. The fabrication process flow of wearable antenna is illustrated in Figure 9. The process flow is similar to the modern fabrication style [33], [34]. Wafer selection plays an important role for the design of wearable antenna, it mainly effects the antenna parameters. 4-inch, P-type, double side polished, 300 μm thick, high resistivity (>5000 Ω-cm) Si <100> wafer was used as the substrates to fabricate the antenna. Then, the wafer is diced to $12 \times 12\,\mu m^2$ area die. Afterwards, oxide growth using standard thermal oxidation was preferred for proper dielectric constant of wearable

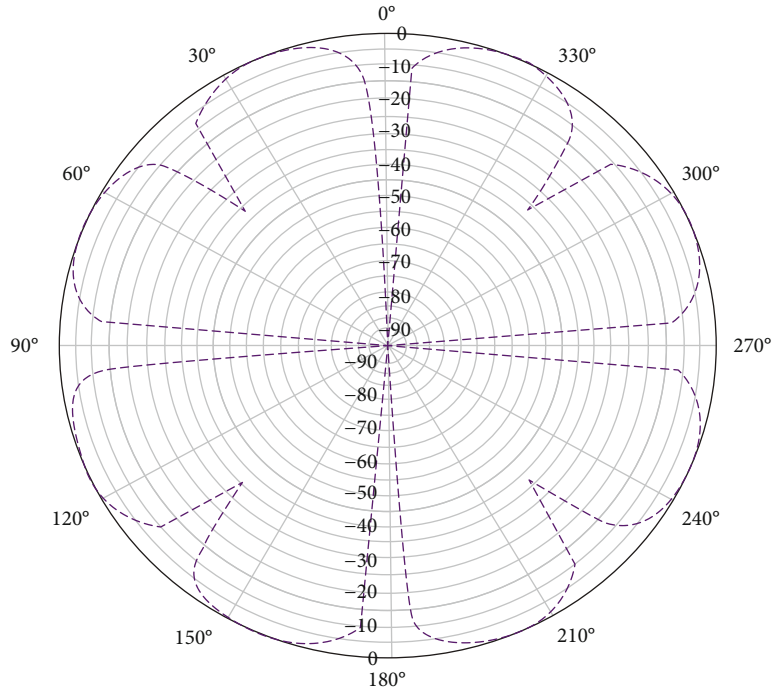

Figure 8: Far field vs. angle for Fmax of dual dipole and patch.

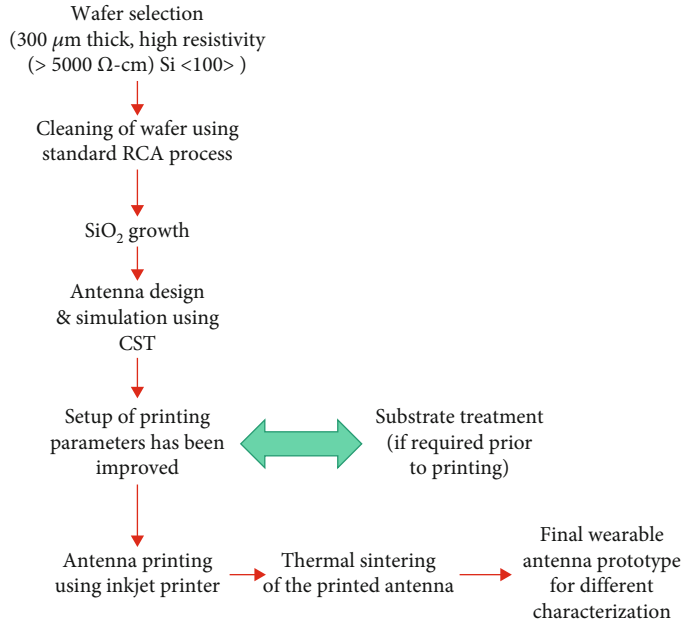

Figure 9: Fabrication process flow for wearable body area network antenna.

antenna. The printing parameters initially can be improved by using simulation. In our work, we have used CST simulator. Inkjet printing has emerged as a viable alternative to traditional production methods like etching and milling. It is an additive technology that allows the design to be directly copied onto the substrate without the use of masks, resulting in reduced waste. Prior to inkjet printing, substrate treatment is preferred.

5. Conclusion

Dynamic apparel body networks will revolutionize the medical stream by aiding in receiving and sending data. In sending block, signal intensifier associated with the transmitter will enhance the signal strength. At reception, a low commotion intensifier associated with the reception apparatus will acquire the signal and will be sent to the end device. A dynamic

polarized antenna has been constructed and analysed in this paper. The gain of the antenna is 13 ± 2 dB for the frequency range of 390 to 610 MHz. Ultrawideband printed antenna might be utilized in medical IoT applications. All radio wires introduced in this paper are minimal wideband dynamic receiving wires for getting and sending wearable speech-enabled IoT device and 5G correspondence frameworks for clinical application in an effective manner. Wearable innovation gives an amazing new apparatus to clinical and careful recovery administrations. A complete analysis using the acquired data will be aided by early detection of anomalous conditions, regulated restoration, and possible information. A dynamic polarized antenna is built, analysed, and attempted production in this paper. For the frequency range of 390 to 610 MHz, the antenna gain is 13 2 dB. The output of the polarized antenna is roughly 19 dBm. The reduced tunable radio wire data transmission is around 14% for a reflection coefficient lower than -9 dB. The tunable receiving wire gain is around 3dBi. Hence, the results of this work are satisfying the current medical needs for the silicon wearable antenna in applications such as pacemakers and health monitoring system.

Data Availability

The data used to support this study are included within the article.

Ethical Approval

This article does not contain any studies with human or animal subjects.

Disclosure

A preprint of the manuscript has previously been published [7]. The publication of this research work is only for the academic purpose of Adama Science and Technology University, Ethiopia.

Conflicts of Interest

The authors declare that they have no conflict of interest regarding the publication of this paper.

Acknowledgments

The authors are thankful to GRIET, Hyderabad, and Adama Science and Technology University, Ethiopia, for their cooperation and support during this research work.

References

[1] M. A. S. Tajin, O. Bshara, Y. Liu, A. Levitt, G. Dion, and K. R. Dandekar, "Efficiency measurement of the flexible on-body antenna at varying levels of stretch in a reverberation chamber," *IET Microwaves, Antennas & Propagation*, vol. 14, no. 3, pp. 154–158, 2020.

[2] S. Kanithan, N. A. Vignesh, S. Jana, C. G. Prasad, E. Konguvel, and S. Vimalnath, "Negative capacitance ferroelectric FET based on short channel effect for low power applications," *SILICON*, 2022.

[3] S. Anthoniraj, K. Saravanan, A. S. Vinay Raj, and N. A. Vignesh, "Optimal design and performance analysis of vertically stacked nanosheet tunnel field effect transistor," *SILICON*, 2022.

[4] H. Li, L. Kang, F. Wei, Y. M. Cai, and Y. Z. Yin, "A low-profile dual-polarized microstrip antenna array for dual-mode OAM applications," *IEEE Antennas and Wireless Propagation Letters*, vol. 16, pp. 3022–3025, 2017.

[5] R. Kumar, B. A. Devi, V. Sireesha et al., "Analysis and Design of Novel Doping Free Silicon Nanotube TFET with High-density Meshing Using ML for Sub Nanometre Technology Nodes," *Silicon*, pp. 1–8, 2022.

[6] S. Kanithan, S. Anthoniraj, P. Manikandan et al., "Temperature influence on dielectric tunnel FET characterization and subthreshold characterization," *SILICON*, 2022.

[7] https://assets.researchsquare.com/files/rs-825439/v1/7d50ca64-4c2d-4be4-8688-dd81e0927f97.pdf?c=1642785792..

[8] K. Fan, Z. C. Hao, Q. Yuan, J. Hu, G. Q. Luo, and W. Hong, "Wideband horizontally polarized omnidirectional antenna with a conical beam for millimeter-wave applications," *IEEE Transactions on Antennas and Propagation*, vol. 66, no. 9, pp. 4437–4448, 2018.

[9] H. J. Lam and J. Bornemann, "Ultra-wideband printed-circuit array antenna for medical monitoring applications," in *In 2009 IEEE International Conference on Ultra-Wideband*, pp. 506–510, IEEE, 2009, September.

[10] K. N. Paracha, S. K. A. Rahim, P. J. Soh et al., "A low profile, dual-band, dual polarized antenna for indoor/outdoor wearable application," *IEEE Access*, vol. 7, pp. 33277–33288, 2019.

[11] H. H. M. Ghouz, M. F. A. Sree, and M. A. Ibrahim, "Novel wideband microstrip monopole antenna designs for WiFi/LTE/WiMax devices," *IEEE Access*, vol. 8, pp. 9532–9539, 2020.

[12] Z. Zhang, S. Li, and J. Wang, "Novel microstrip antenna design upon transformation medium," *IEEE Antennas and Wireless Propagation Letters*, vol. 14, pp. 543–546, 2014.

[13] A. Sabban and K. C. Gupta, "Characterization of radiation loss from microstrip discontinuities using a multiport network modeling approach," *IEEE Transactions on Microwave Theory and Techniques*, vol. 39, no. 4, pp. 705–712, 1991.

[14] M. Mosalanejad, I. Ocket, C. Soens, and G. A. Vandenbosch, "Wideband compact comb-line antenna array for 79 GHz automotive radar applications," *IEEE Antennas and Wireless Propagation Letters*, vol. 17, no. 9, pp. 1580–1583, 2018.

[15] R. Kastner, E. Heyman, and A. Sabban, "Spectral domain iterative analysis of single-and double-layered microstrip antennas using the conjugate gradient algorithm," *IEEE transactions on antennas and propagation*, vol. 36, no. 9, pp. 1204–1212, 1988.

[16] G. Zheng, T. Zhi-Hong, Z.-M. Xie, Q.-X. Chu, and Y. Yao, "Compact wideband circularly polarized microstrip antenna array for 45 GHz application," *IEEE Transactions on Antennas and Propagation*, vol. 66, no. 11, pp. 6388–6392, 2018.

[17] L. Xu, M. Q. H. Meng, D. Wei, and H. Ren, "Variation of Radiation Effects and Signal Efficiency with Distance between Electromagnetic Source and Trunk Model," in *In 2007 29th Annual International Conference of the IEEE Engineering in Medicine and Biology Society*, pp. 1184–1187, IEEE, 2007, August.

[18] S.-K. Lee, S. Bulumulla, F. Wiesinger, L. Sacolick, W. Sun, and I. Hancu, "Tissue electrical property mapping from zero echo-time magnetic resonance imaging," *IEEE Transactions on Medical Imaging*, vol. 34, no. 2, pp. 541–550, 2015.

[19] J. Wang, M. Leach, E. G. Lim, Z. Wang, R. Pei, and Y. Huang, "An implantable and conformal antenna for wireless capsule endoscopy," *IEEE Antennas and Wireless Propagation Letters*, vol. 17, no. 7, pp. 1153–1157, 2018.

[20] M. Abdullah and A. Khan, "Multiband wearable textile antenna for ISM body center communication systems," in *In 2015 XXth IEEE International Seminar/Workshop on Direct and Inverse Problems of Electromagnetic and Acoustic Wave Theory (DIPED)*, pp. 90–96, IEEE, 2015, September.

[21] F. Dhaouadi, S. Beldi, R. Bedira, and A. Gharsallah, "Design and performance analysis of complex Planar Triangular Monopole Textile Antenna in vicinity of human body for wearable applications," in *In 2015 IEEE 15th Mediterranean Microwave Symposium (MMS)*, pp. 1–4, IEEE, 2015, December.

[22] J. S. Roh, Y. S. Chi, J. H. Lee, Y. Tak, S. Nam, and T. J. Kang, "Embroidered wearable multiresonant folded dipole antenna for FM reception," *IEEE Antennas and Wireless Propagation Letters*, vol. 9, pp. 803–806, 2010.

[23] B. Shilpa, L. K. Rao, N. A. Vignesh, and V. V. Kumar, "Design of inset fed circular dual band patch antenna for WLAN frequencies," *International Journal of Systems, Control and Communications*, vol. 13, no. 1, pp. 56–66, 2022.

[24] S. Kanithan, N. A. Vignesh, E. Karthikeyan, and N. Kumareshan, "An intelligent energy efficient cooperative MIMO-AF multi-hop and relay based communications for Unmanned Aerial Vehicular networks," *Computer Communications*, vol. 154, pp. 254–261, 2020.

[25] R. Senthilkumar, G. M. Tamilselvan, S. Kanithan, and N. A. Vignesh, "Routing in WSNs powered by a hybrid energy storage system through a CEAR protocol based on cost welfare and route score metric," *International Journal Of Computers Communications & Control*, vol. 14, no. 2, pp. 233–252, 2019.

[26] W. Wang, L. Yang, Q. Zhang, and T. Jiang, "Securing on-body IoT devices by exploiting creeping wave propagation," *IEEE Journal on Selected Areas in Communications*, vol. 36, no. 4, pp. 696–703, 2018.

[27] H. Wang, M. Xu, W. Zhang et al., "Mechanical and biological characteristics of diamond-like carbon coated poly aryl-ether-ether-ketone," *Biomaterials*, vol. 31, no. 32, pp. 8181–8187, 2018.

[28] S. W. Ellingson, J. H. Simonetti, and C. D. Patterson, "Design and evaluation of an active antenna for a 29–47 MHz radio telescope array," *IEEE Transactions on Antennas and Propagation*, vol. 55, no. 3, pp. 826–831, 2007.

[29] J. W. Hand, G. M. J. Van Leeuwen, S. Mizushina et al., "Monitoring of deep brain temperature in infants using multi-frequency microwave radiometry and thermal modelling," *Physics in Medicine and Biology*, vol. 46, no. 7, pp. 1885–1903, 2001.

[30] S. P. Sugumar, K. Arunachalam, and C. V. Krishnamurthy, "Design of an Ultra-wide Band Active Antenna for Medical Microwave Radiometry," in *2019 URSI Asia-Pacific Radio Science Conference (AP-RASC)*, pp. 1–3, IEEE, 2019, March.

[31] K. Chang, R. A. York, P. S. Hall, and T. Itoh, "Active integrated antennas," *IEEE transactions on microwave theory and techniques*, vol. 50, no. 3, pp. 937–944, 2002.

[32] J. D. McKinney, I. S. Lin, and A. M. Weiner, "Shaping the power spectrum of ultra-wideband radio-frequency signals," *IEEE Transactions on Microwave Theory and Techniques*, vol. 54, no. 12, pp. 4247–4255, 2006.